


RAI14 Regulated by circNFATC3/miR-23b-3p axis Facilitates Cell Growth and Invasion in Gastric Cancer

Cell Transplantation
Volume 30: 1–10
© The Author(s) 2021
Article reuse guidelines:
sagepub.com/journals-permissions
DOI: 10.1177/09636897211007055
journals.sagepub.com/home/ctj


XinXin Yan^{1,2} , MingZhi Zhang^{1,3}, BingBing Li⁴, Xia Ji⁴, HongJin Wu⁵, and QingYu Zhang¹

Abstract

Circular RNAs (circRNAs) have been proved to act crucial roles in multiple malignancies including gastric cancer (GC). Retinoic acid induced 14 (RAI14) acts as an oncogene in human cancers, but the underlying mechanisms by which RAI14 is regulated by circRNA/miRNA axis remain elusive. The clinical value of RAI14, miR-23b-3p and circNFATC3 was estimated by The Cancer Genome Atlas and fluorescence in situ hybridization. The interplay between miR-23b-3p and RAI14 or circNFATC3 was determined by qRT-PCR, Western blot, luciferase gene report and RIP assays. Biological function assays and a subcutaneous xenograft model were executed to unveil the role of circNFATC3/miR-23b-3p/RAI14 axis in GC cells. As a consequence, upregulation of RAI14 and circNFATC3 or downregulation of miR-23b-3p was associated with poor prognosis in patients with GC. Restored miR-23b-3p depressed cell proliferation, colony formation, and cell invasion by targeting RAI14, whereas RAI14 facilitated cell progression and reversed the anti-tumor effects of miR-23b-3p in GC cells. Then, circNFATC3 had a co-localization with miR-23b-3p in the cytoplasm in GC tissue cells and could act as a sponge of miR-23b-3p in GC cell line. Silencing of circNFATC3 inhibited cell growth and in vivo tumorigenesis by upregulating miR-23b-3p and downregulating RAI14. In conclusion, our findings indicated that RAI14 facilitated cell growth and invasion and was regulated by circNFATC3/miR-23b-3p axis in GC.

Keywords

RAI14, circNFATC3, miR-23b-3p, growth, gastric cancer

Introduction

Gastric cancer (GC) is considered as the third most common cancer and the third leading causes of cancer death in China¹. In spite of the great progress in the diagnosis and treatment of GC including eradication of helicobacter pylori and resection of early GC², the advanced patients still harbor an unfavorable prognosis due to the tumor infiltration and metastasis³. Recent studies have shown that the pathogenesis of GC is related to the dysregulation of coding RNAs or non-coding RNAs^{4,5}. Identification of these potential biomarkers may be beneficial for the early detection of GC.

Retinoic acid induced 14 (RAI14) is a protein-coding gene first found in human retinal pigment epithelial cells and induced by all-trans-retinoic acid⁶. RAI14 has been reported to participate in regulating f-actin dynamics at the ectoplasmic specialization in the rat testis⁷ and predict chemotherapy survival in lung and breast cancers⁸. RAI14 is upregulated in GC⁹ and breast cancer¹⁰, represents an independent predictor of poor survival in GC⁹ and enhances

mTOR-mediated inflammation in glioblastoma¹¹, while knockdown of RAI14 represses the growth and invasion by inactivating AKT signaling in GC¹² and breast cancer¹⁰.

¹ Department of Gastroenterology, Tianjin Medical University General Hospital, Tianjin, China

² Department of Geriatric, Aerospace Center Hospital, Peking University Aerospace School of Clinical Medicine, Beijing, China

³ Department of Gastroenterology, The third affiliated hospital of Jinzhou Medical University, Jinzhou, China

⁴ Department of Gastroenterology, The Second Affiliated Hospital of Jiaxing University, Jiaxing, Zhejiang, China

⁵ Central Laboratory for Science and Technology, Longhua hospital, Shanghai University of traditional Chinese Medicine, Shanghai, China

Submitted: March 14, 2021. Revised: March 14, 2021. Accepted: March 14, 2021.

Corresponding Author:

QingYu Zhang, Department of Gastroenterology, Tianjin Medical University General Hospital, No.154, Anshan Road, Tianjin 300052, China. Email: zhangqy@tmu.edu.cn



Creative Commons Non Commercial CC BY-NC: This article is distributed under the terms of the Creative Commons Attribution-NonCommercial 4.0 License (<https://creativecommons.org/licenses/by-nc/4.0/>) which permits non-commercial use, reproduction and distribution of the work without further permission provided the original work is attributed as specified on the SAGE and Open Access pages (<https://us.sagepub.com/en-us/nam/open-access-at-sage>).

Circular RNAs (circRNAs) is a novel subset of non-coding RNAs characterized by a closed loop structure, a resistance to RNase R and high conservativity¹³. Increasing evidence has shown that circRNAs can sponge multiple miRNAs involved in GC progression¹⁴. For example, circLMTK2¹⁵, circDLST¹⁶ and CiRS-7¹⁷ can sponge miR-150-5p, miR-502-5p, and miR-7 to prompt GC cell proliferation and metastasis, while CircPSMC3¹⁸, circFAT1(e2)¹⁹, and circLARP4²⁰ sponge miR-296-5p, miR-548 g, and miR-424-5p to repress GC tumorigenesis and progression. Moreover, upregulation of circLMTK2¹⁵ and circDLST¹⁶ or downregulation of circPSMC3¹⁸ indicates a poor prognosis and lymph node metastasis in patients with GC.

Previous study showed that RAI14 is negatively regulated by miR-653-5p and promotes melanoma progression²¹, and miR-103 facilitates porcine preadipocyte differentiation in pigs by targeting RAI14²². Herein, we found that the dysregulation of RAI14, miR-23b-3p, and circNFATC3 was linked to a poor prognosis in patients with GC. Ectopic miR-23b-3p repressed GC cell growth and invasion by targeting RAI14. Moreover, hsa_circ_0039930 (also termed as circNFATC3), predominantly localized in the cytoplasm, could act as a sponge of miR-23b-3p to upregulate RAI14, thereby leading to GC tumorigenesis.

Materials and Methods

Clinical Sample

The clinical data for GC as well as the expression levels of RAI14 and 13 miRNAs (miR-9-5p, miR-23a-3p, miR-23b-3p, miR-23c, miR-103a-3p, miR-107, miR-130a-3p, miR-301a-3p, miR-324-5p, miR-372-3p, miR-376c-3p, miR-410-3p, miR-504-5p) in GC tissue samples were downloaded from TCGA dataset (<http://xena.ucsc.edu/>). In addition, a tissue microarray consisting of 90 GC tissue samples (Lot No. XT17-035) was purchased from Outdo Biotech Company (Shanghai, China). 10 paired GC frozen tissues were stored in our laboratory and 10 paired tissue sections were from Department of Pathology. The study was approved by the Ethics Committee of Beijing Aerospace Center Hospital (No. 2021-ASCH-002).

Cell Culture

GES-1 and GC cell lines (MKN-28, MGC-803, SGC-7901, BGC-823, AGS) were stored in our laboratory and cultured in Dulbecco's Modified Eagle medium (DMEM) medium supplemented with 10% heat-inactivated fetal bovine serum (FBS).

FISH Analysis

Biotin-labeled probe sequence for miR-23b-3p (5'-GTGG TAATCCCTGGCAATGTG AT-3') and digoxin-modified probe sequence for hsa_circ_0039930 (circNFATC3,

5'-GTAATGAAGATGTGCTTCACAACAGGAT-3') were executed for FISH analysis of their expression levels and colocalization in GC tissues. The detailed description of FISH analysis and quantification was conducted as previously reported¹⁶.

Quantitative Real-Time PCR (qRT-PCR)

The qRT-PCR analysis was executed as previously reported¹⁶. The primer sequences used in this study were listed in Supplemental Table S1.

Western Blot Analysis

MKN-28 and AGS cell lines were harvested and extracted by using lysis buffer. The anti-RAI14 (17507-1-AP, Proteintech, Rosemont, IL, USA) was diluted at a ratio of 1:1000 according to the instructions and incubated overnight at 4°C. The detailed description of Western blot analysis was executed as previously reported¹⁶.

Luciferase Reporter Assay

MKN-28 and AGS cell lines were seeded into 96-well plates and co-transfected with a mixture of pGL3-Promoter luciferase reporter containing wild type (WT) and mutant (Mut) RAI14 3'UTR or circNFATC3 3'UTR and miR-23b-3p mimic or inhibitor. The luciferase activities of WT and Mut RAI14 3'UTR were examined with a dual-luciferase reporter assay.

The Lentivirus, siRNA, miR-23b-3p Mimic and Inhibitor

RAI14 plasmids, siRNA targeting RAI14 (si-RAI14: 5'-CAGAGTACATCA AGAAGCTTCTTCA-3'), lentivirus-mediated circNFATC3, or sh-circNFATC3 (interference sequence: 5'-CTGTTGTGAA GCACATCTTCA-3') and miR-23b-3p mimic/inhibitor were purchased from GenePharma (Shanghai, China). Negative control plasmids or lentiviruses (NC) and miR-NC were used as the control vectors.

MTT, Colony Formation and Transwell Assays

MTT, colony formation and Transwell assays were conducted as previously described¹⁶.

CircRNA Expression Profiling

The detailed description of the circRNA expression profiling between GC and adjacent normal tissues ($n = 3$) was conducted as previously reported²⁰.

RNase R Treatment

Total RNA from the MKN-28 and AGS cell lines was incubated for 30 min at 37°C with 3U/μg of RNase R

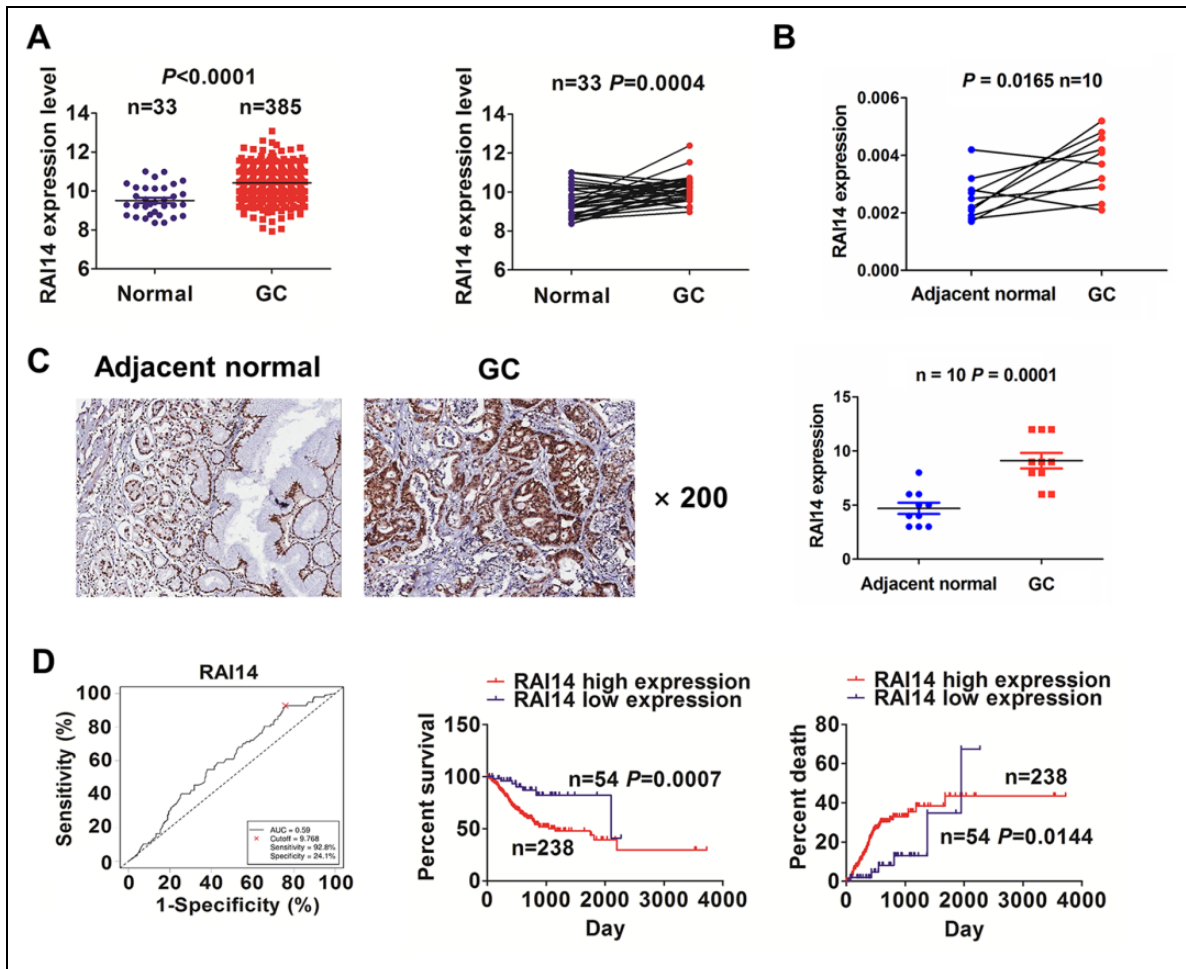


Figure 1. The association of RAI14 expression with poor prognosis in patients with GC. (A) TCGA analysis of the expression levels of RAI14 in unpaired ($n = 385$) and paired ($n = 33$) GC tissue samples. (B) qRT-PCR analysis of the expression levels of RAI14 in paired ($n = 10$) GC tissue samples. (C) IHC analysis of the expression levels of RAI14 in paired ($n = 10$) GC tissue samples. (D) ROC curve analysis of the cutoff value, sensitivity, specificity, and AUC of RAI14 in GC patients and Kaplan Meier analysis of the association of high or low RAI14 expression with the overall survival and tumor recurrence in patients with GC.

(Epicentre Technologies, Madison, WI, USA). The enrichment levels of circNFATC3 and NFATC3 in MKN-28 and AGS cells were detected by qRT-PCR analysis.

RNA Immunoprecipitation (RIP)

RIP assay was performed in MKN-28 cell line by using a Magna RIP RNA-binding protein Immunoprecipitation Kit (Millipore) according to the manufacturer's instructions. Antibodies for RIP assays against Ago2 and IgG were purchased from Abcam (ab5072, Rabbit polyclonal antibody, Cambridge, MA, USA).

In vivo Tumorigenesis Assay

Male BALB/c nude mice (4–5 week old) were purchased from Shanghai SIPPR-BK Laboratory Animal Co. Ltd (Shanghai, China). All the animals used were approved by

the Animal Ethics Committee of Beijing Aerospace Center Hospital (No. 2021-ASCH-002). The mice were subcutaneously inoculated with 1×10^7 of MKN-28 cells stably transfected with si-circNFATC3 or si-NC. The body weight and tumor size were examined, and the tumor volume was calculated according to the formula: length \times width²/2.

Immunohistochemistry (IHC) Analysis

IHC analysis of Ki-67 and RAI14 protein levels was executed on paraffin slides of nude mice GC tissues using anti-Ki-67 (Abcam, Cambridge, UK) and anti-RAI14 antibodies (17507-1-AP, Proteintech, Rosemont, IL, USA). The detailed description of IHC was executed as previously reported²⁰.

Statistical Analysis

Statistical analysis was executed as previously reported¹⁶. The data analyses were executed by using SPSS 20.0 (IBM,

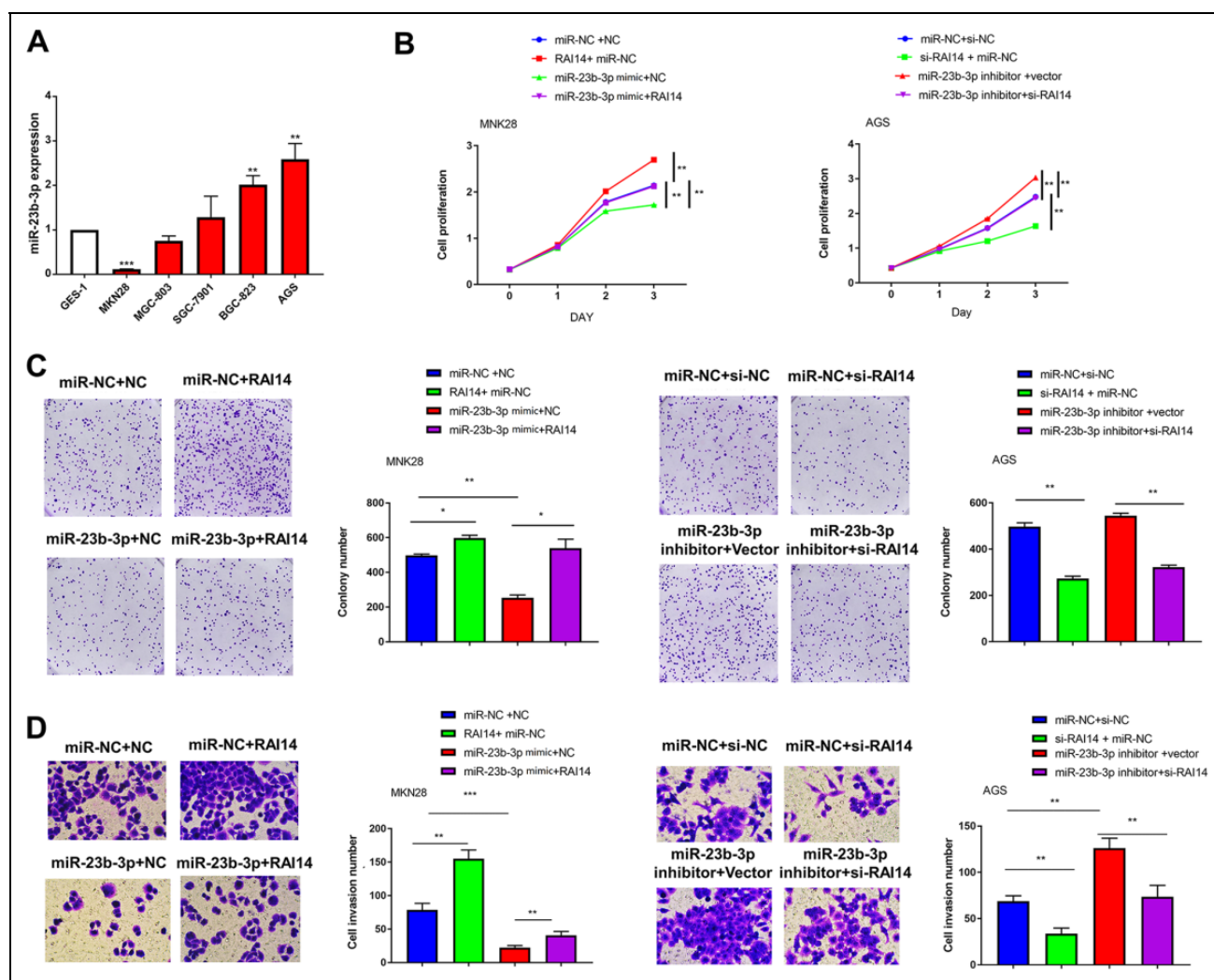


Figure 2. RAI14 promoted cell growth and invasion and reversed the anti-tumor effects of miR-23b-3p in GC cells. (A) MTT, (B) colony formation, and (C) Transwell assay were conducted for assessing the cell viability, colony formation number and invasive potential after the co-transfection with miR-23b-3p mimic and RAI14 plasmids in MKN-28 cells or miR-23b-3p inhibitor and si-RAI14 in AGS cells. Data are the means \pm SEM of three experiments. * $P < 0.05$; ** $P < 0.01$; *** $P < 0.001$.

SPSS, Chicago, IL, USA) and GraphPad Prism. Student's t-test or Chi-square test was used to assess the statistical significance for comparisons of two groups. The Pearson's correlation coefficient analysis was used to analyze the correlations. The association of RAI14, miR-23b-3p, and circNFATC3 with the prognosis of GC was conducted by Kaplan-Meier method. Univariate analysis and multivariate models were performed by using a Cox proportional hazards regression model. $P < 0.05$ was considered statistically significant.

Results

Upregulation of RAI14 Was Associated with Poor Prognosis in Patients with GC

According to the TCGA analysis, it was found that RAI14 expression was dramatically upregulated in

unpaired ($n = 385$, $P < 0.0001$) and paired ($n = 33$, $P < 0.0001$) GC tissue samples (Fig. 1A). This result was further validated in paired GC tissues or sections by qRT-PCR (Fig. 1B) and IHC analyses (Fig. 1C). In the light of the survival time and status, a cutoff value of RAI14 (9.768) was acquired in patients with GC and divided the patients into RAI14-high and RAI14-low groups (Fig. 1D). The high expression of RAI14 had no correlation with the clinicopathological characteristics ($P > 0.05$) in GC (Supplemental Table S2). The patients with RAI14-high expression possessed a poorer survival ($P = 0.0007$) and a higher tumor recurrence ($P = 0.014$) as compared with RAI14-low expression (Fig. 1D). Cox regression analysis demonstrated that high expression of RAI14 was an independent prognostic factor for poor survival (Supplemental Table S3) and tumor recurrence (Supplemental Table S4) in patients with GC.

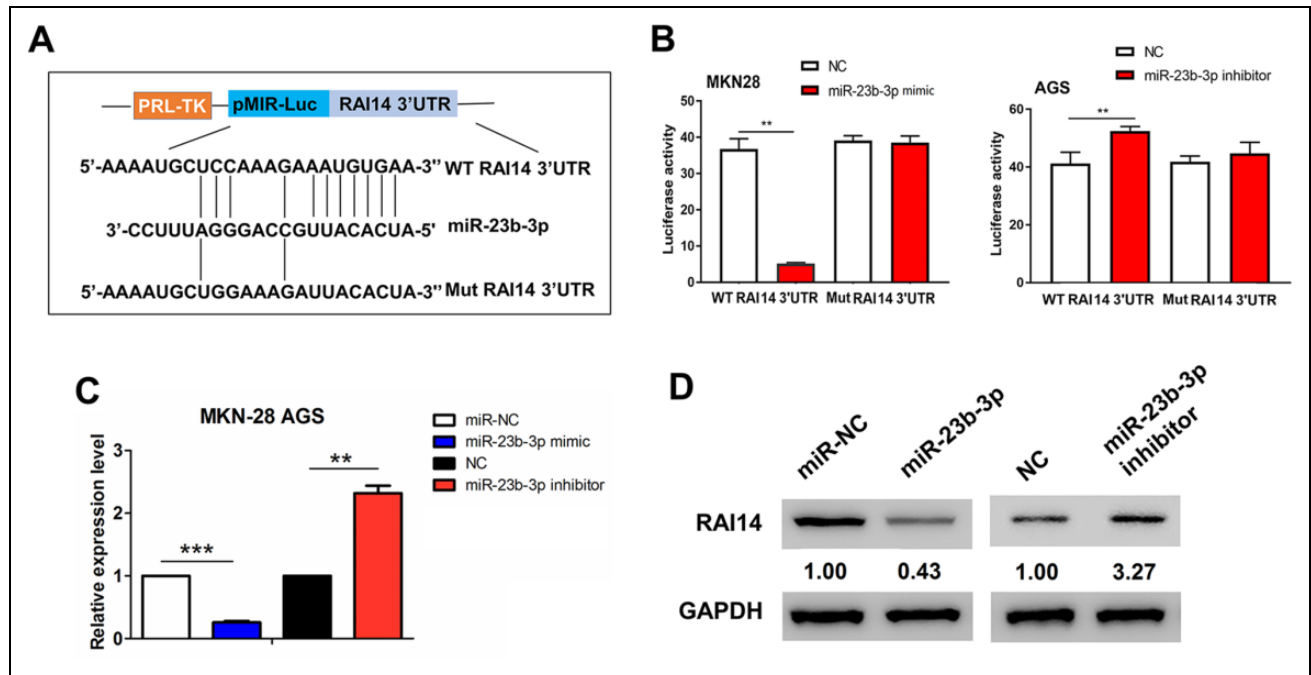


Figure 3. RAI14 was a direct target of miR-23b-3p in GC cells. (A) The binding sites between RAI14 3'UTR and miR-23b-3p. (B) The activity of WT or Mut RAI14 3'UTR after the treatment with miR-23b-3p mimic in MKN-28 cells or miR-23b-3p inhibitor in AGS cells. (C, D) qRT-PCR and Western blot analysis of the expression levels of RAI14 after the treatment with miR-23b-3p mimic in MKN-28 cells or miR-23b-3p inhibitor in AGS cells. Data are the means \pm SEM of three experiments. ** $P < 0.01$; *** $P < 0.001$.

miR-23b-3p Was Negatively Correlated with RAI14 Expression in GC

It was shown that upregulated of RAI14 had no correlation with its methylation levels in GC (Supplemental Fig. S1). Whether RAI14 expression was negatively regulated by miRNAs at a post-transcriptional level was observed. A starBaseV2.0 website (<http://starbase.sysu.edu.cn/starbase2/index.php>) was used to identify 13 miRNAs which have the strongest binding potential with RAI14 3' UTR. The expression levels of these miRNAs were validated in unpaired (Supplemental Fig. S2A) and pair-matched tissue samples (Supplemental Fig. S2B), and miR-23b-3p and miR-9-5p harbored a dramatical downregulation in GC tissues, and only miR-23b-3p had a negative correlation with RAI14 expression in GC tissues ($n = 360$, Supplemental Fig. S2C). Then, a cutoff value of miR-23b-3p was obtained in GC and the patients with miR-23b-3p-high expression had a longer survival as compared with miR-23b-3p-low expression (Supplemental Fig. S2D).

RAI14 Promoted Cell Growth and Invasion and Reversed the Anti-Oncogenic Effects of miR-23b-3p in GC

The expression levels of RAI14 in varied GC cell lines were determined by qRT-PCR analysis, which indicated that RAI14 harbored a higher expression in AGS cell line but a lower expression in MKN-28 cell line as compared

with the GES-1 cell line (Fig. 2A). The overexpression efficiencies of RAI14 plasmids in MKN-28 or the knock-down efficiencies of si-RAI14 in AGS were respectively confirmed by qRT-PCR and Western blot analysis (Supplemental Fig. S3A). Likewise, the treatment efficiencies of miR-23b-3p mimic in MKN-28 or its inhibitor in AGS were determined by qRT-PCR analysis (Supplemental Fig. S3B). It was found that ectopic expression of RAI14 facilitated cell proliferation (Fig. 2B), colony formation (Fig. 2C) and cell invasion (Fig. 2D), and reversed the inhibitory effects of miR-23b-3p mimics in MKN-28 cell line, whereas knockdown of RAI14 had the opposite effects in AGS cell line (Fig. 2B–D).

RAI14 was Identified as a Direct Target of miR-23b-3p in GC

Having confirmed a negative correlation of miR-23b-3p with RAI14 in GC, we validated whether RAI14 was a direct target of miR-23b-3p in GC. The binding sites between miR-23b-3p and RAI14 3'UTR were indicated in Fig. 3A. Luciferase reporter vectors containing WT or Mut RAI14 3'UTR were transfected with miR-23b-3p mimics in MKN-28 cells or miR-23b-3p inhibitor in AGS cells. The results indicated that the luciferase activity of WT RAI14 3'UTR was lowered by miR-23b-3p in MKN-28 cells, and increased by miR-23b-3p inhibitor in AGS cells, but that of Mut RAI14 3'UTR was unaffected by miR-23b-3p mimics or inhibitor in GC cells (Fig. 3B). Then, miR-23b-3p mimics decreased the expression of

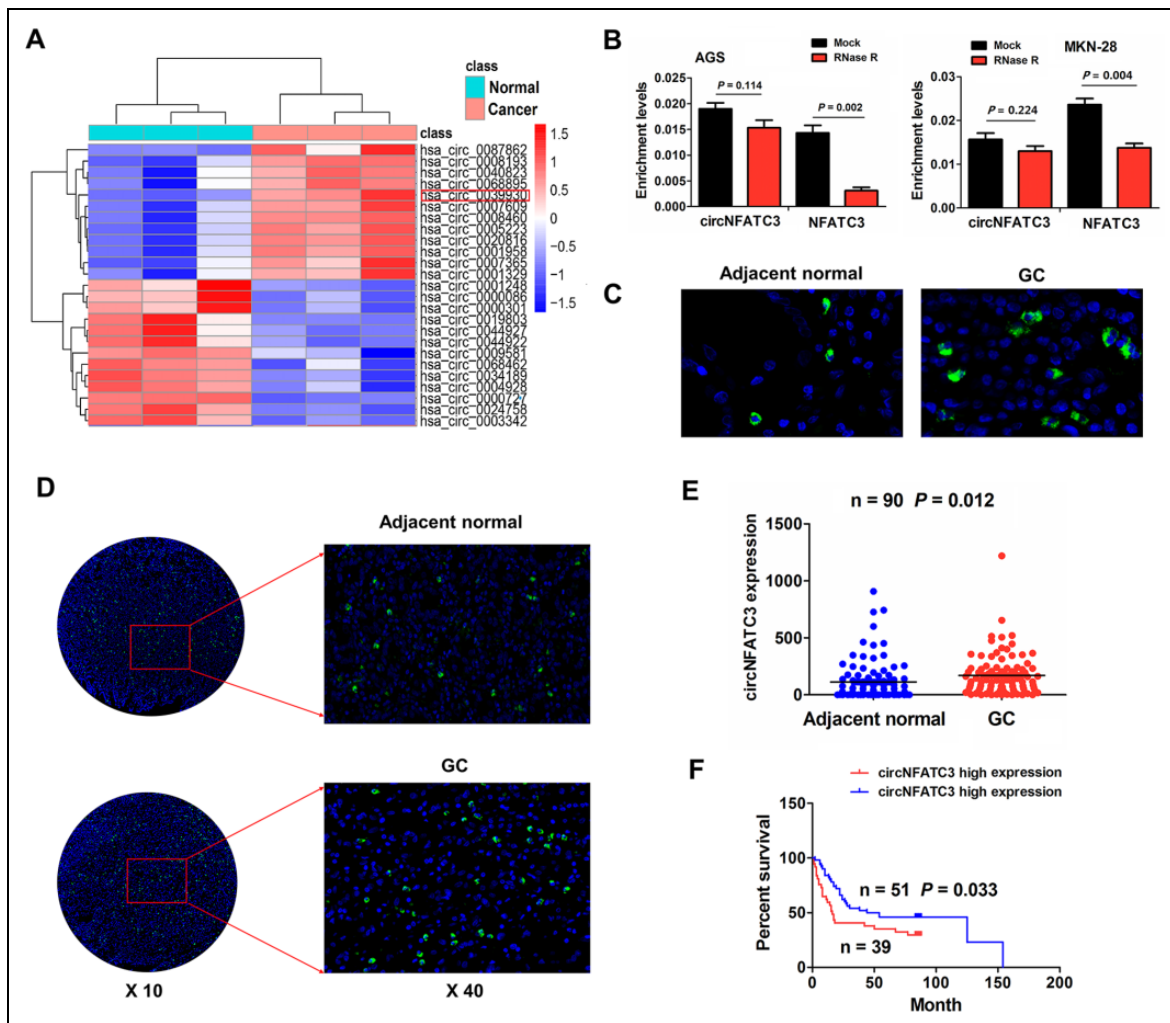


Figure 4. A novel circNFATC3 was identified to harbor a poor prognosis in GC. (A) circRNA expression profiling analysis of the differentially expressed circRNAs between GC and adjacent normal tissues. (B) qRT-PCR analysis of the enrichment levels of circNFATC3 and NFATC3 after exposure to RNase R in MKN-28 and AGS cell lines. (C) FISH analysis of the cellular localization of circNFATC3 in GC and adjacent normal tissues. The nuclei were stained with DAPI for blue color, and circNFATC3 in the cytoplasm was stained for green color. (D, E) FISH analysis of the expression levels of circNFATC3 in 90 paired GC tissues samples. (F) Kaplan Meier analysis of the association of high or low circNFATC3 expression with the overall survival in patients with GC. Data are the means \pm SEM of three experiments.

RAI14 in MKN-28, whereas its inhibitor increased RAI14 expression in AGS cells (Fig. 3C, D).

A Novel circNFATC3 Was Identified to Harbor a Poor Survival in GC

According to the miRbase and circRNA expression profiling (Fig. 4A), we identified 12 upregulated circRNAs and 13 downregulated circRNAs in GC tissues ($P < 0.03$ and $FC > 3$) and found that hsa_circ_0039930 harbored a marked upregulation in GC ($P = 0.002$ and $FC = 8.50$). hsa_circ_0039930 is derived from the exon regions within nuclear factor of activated T cells 3 (NFATC3) locus, and is termed as circNFATC3. To confirm the loop structure and stability of circNFATC3 in GC cells, we treated the GC cells with RNase R and found that circNFATC3

produced a resistance to RNase R treatment in contrast with linear NFATC3 in MKN-28 and AGS (Fig. 4B). FISH analysis showed that circNFATC3 was mainly localized in the cytoplasm of GC and normal tissue cells (Fig. 4C). FISH analysis further validated that the expression of circNFATC3 was increased in GC tissues as compared with the adjacent normal tissues (Fig. 4D, E). Then, we found that the patients with circNFATC3-high expression possessed a shorter survival as compared with circNFATC3-low expression (Fig. 4F).

Knockdown of circNFATC3 Repressed Cell Growth by Regulating miR-23b-3p/RAI14 Axis in GC Cells

The silencing efficiencies of si-circNFATC3 was determined in MKN-28 cells by qRT-PCR (Fig. 5A). It was

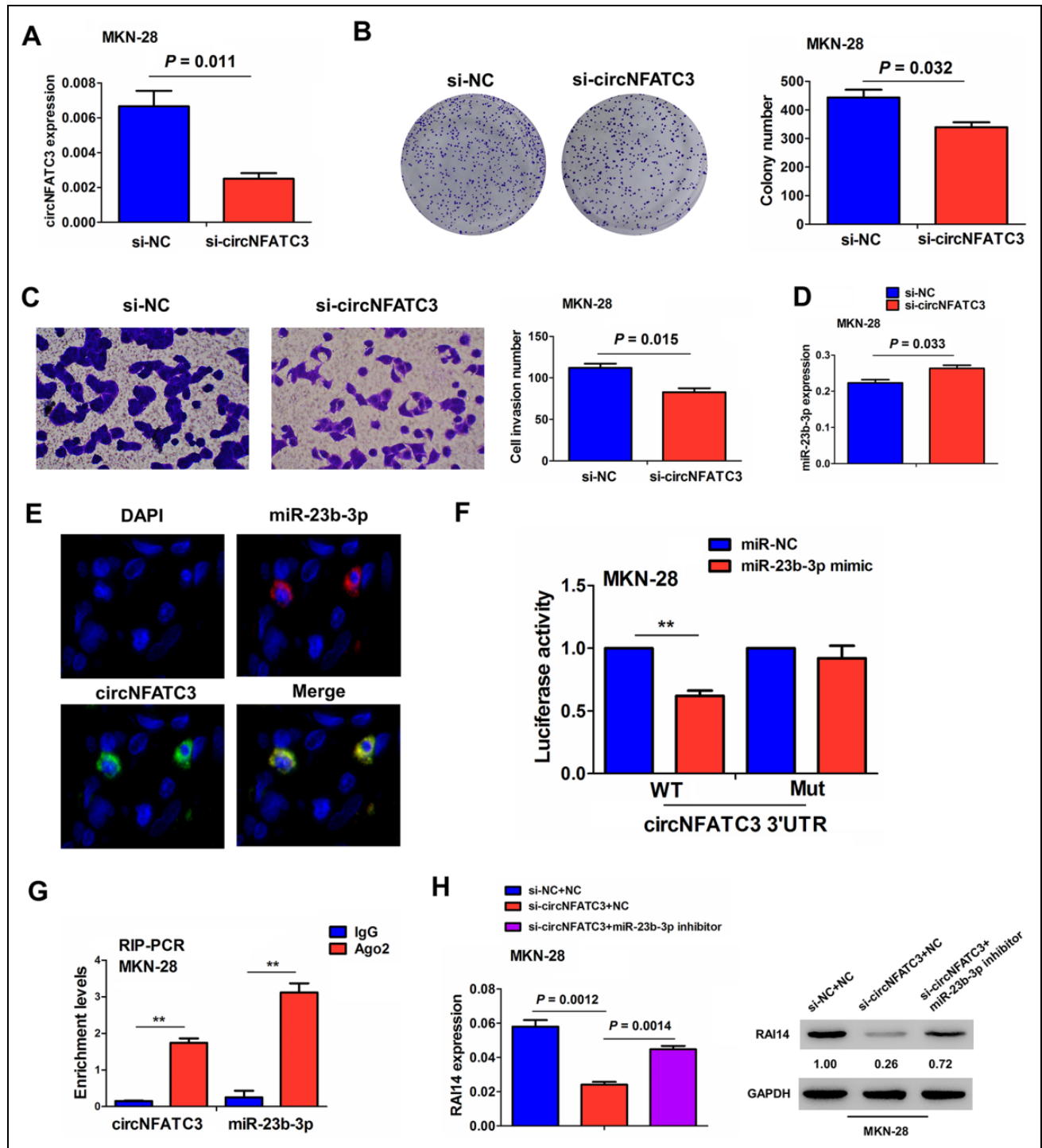


Figure 5. Knockdown of circNFATC3 repressed cell growth and invasion by regulating miR-23b-3p/RAI14 axis in GC cells. (A) qRT-PCR analysis of the silencing efficiencies of si-circNFATC3 in MKN-28 cells. (B) Colony formation and (C) Transwell assay were conducted for assessing the colony formation number and invasive potential after the transfection with si-circNFATC3 in MKN-28 cells. (D) qRT-PCR analysis of the effects of circNFATC3 knockdown on miR-23b-3p expression in MKN-28 cells. (E) FISH analysis of the co-localization of circNFATC3 and miR-23b-3p in GC tissue cells. (F) Luciferase report assay indicated the effects of miR-23b-3p mimics on the luciferase activities of WT or Mut circNFATC3 3'UTR in MKN-28 cells. (G) RIP-PCR analysis of the amount of circNFATC3 and miR-23b-3p pulled down from Ago2 or IgG protein in MKN-28 cells. (H) qRT-PCR and Western blot analysis of the effects of the co-transfection with si-circNFATC3 and miR-23b-3p inhibitor on RAI14 expression in MKN-28 cells. Data are the means \pm SEM of three experiments.

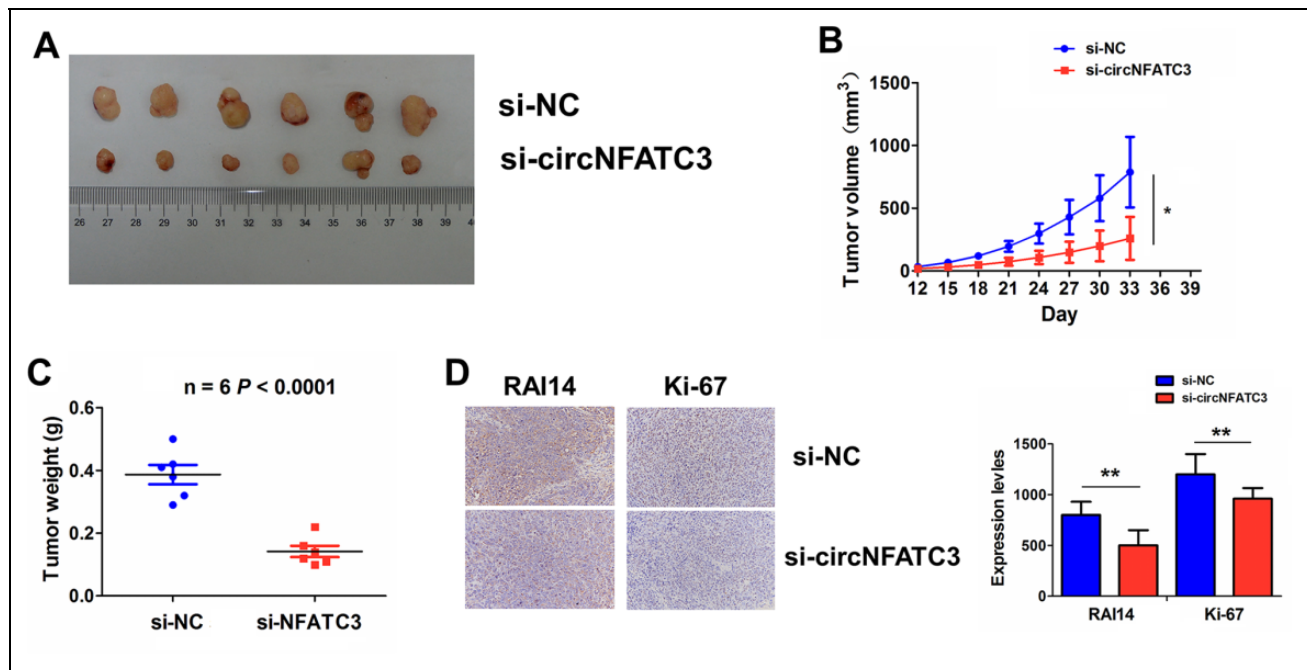


Figure 6. Knockdown of circNFATC3 repressed in vivo tumorigenesis of GC. (A, B) A growth curve analysis of the tumor growth in si-circNFATC3 or si-NC transfected MKN-28 cells. (C) Comparison of the tumor weight of xenograft tumors induced by si-circNFATC3 or si-NC transfected MKN-28 cells. (D) IHC analysis of the protein levels of RAI14 and Ki-67 in tumor tissues induced by si-circNFATC3 or si-NC transfected MKN-28 cells. ** $P < 0.01$.

shown that knockdown of circNFATC3 repressed the colony formation (Fig. 5B) and cell invasion (Fig. 5C), followed by the decreased expression of miR-23b-3p in MKN-28 cells (Fig. 5D). However, knockdown of circNFATC3 exerted no effects on cell growth and invasion in AGS cells (Supplemental Fig. S4). According to the predict outcomes from the circRNA profiling and miRbase, circNFATC3 had the potential to bind with miR-23b-3p. FISH analysis showed that circNFATC3 harbored a colocalization with miR-23b-3p in the cytoplasm of GC tissue cells (Fig. 5E). The binding sites between circNFATC3 and miR-23b-3p were demonstrated in Supplemental Fig. S5. Luciferase report assay showed that miR-23b-3p could bind with circNFATC3 3'UTR and reduce its WT activities instead of the Mut activities in MKN-28 cells. qPCR indicated that knockdown of circNFATC3 increased miR-23b-3p expression levels (Fig. 5F). RIP assay was executed for Ago2 in MKN-28 cells and the expression level of endogenous circNFATC3 and miR-23b-3p pulled-down from Ago2-expressed MKN-28 cells was detected by qRT-PCR analysis, indicating that, circNFATC3 and miR-23b-3p were highly enriched in the Ago2 pellet as compared with those in the input control (Fig. 5G). In addition, knockdown of circNFATC3 decreased the expression of RAI14, but miR-23b-3p inhibitor reversed the inhibitory effects of circNFATC3 knockdown on RAI14 expression in MKN-28 cells (Fig. 5H).

Knockdown of circNFATC3 Repressed in vivo Tumorigenesis of GC

To confirm the effects of circNFATC3 on GC in vivo tumorigenesis, a xenograft tumor model was established after subcutaneous inoculation with si-circNFATC3 or si-NC stably transfected MKN-28 cells. It was found that the volumes of GC tumors were smaller in circNFATC3 group in comparison with si-NC group (Fig. 6A, B). After GC tumor tissues were harvested, the average tumor weight was also slighter in si-circNFATC3 group than that in si-NC group (Fig. 6C). IHC analysis showed that the protein levels of RAI14 and Ki-67 were significantly reduced in circNFATC3 group in comparison with si-NC group (Fig. 6D).

Discussion

Increasing data indicate that RAI14 expression is elevated in GC⁹ and breast cancer¹⁰ and displays a poor survival in GC⁹. But, the correlation of RAI14 expression with tumor recurrence in GC remains unreported. In the present study, it was validated that RAI14 expression levels were not only increased in GC samples, but also acted as an independent prognostic of poor survival and tumor recurrence in patients with GC. Restored RAI14 facilitated GC cell proliferation, colony formation and cell invasion. These results suggested that RAI14 might be a promising predictor or an oncogenic factor in GC.

We then found that the upregulation of RAI14 in GC tissue samples was attributable to the post-transcriptional regulation of miR-23b-3p in GC rather than the epigenetic modification. It has been reported that, on the one hand, the tissue levels of miR-23b-3p are decreased and act as a predictor in hepatocellular carcinoma²³ and GC and miR-23b-3p reverses chemotherapy resistance in GC by targeting ATG12 and HMGB2²⁴. On the other hand, the serum or tissue levels of miR-23b-3p are increased in non-small cell lung cancer²⁵, osteosarcoma²⁶, and esophageal squamous cell carcinomas²⁷, and miR-23b-3p promotes tumor proliferation and metastasis by targeting PGC1 α or EBF3^{26,27}. In the present study, low expression of miR-23b-3p indicated a poor survival in GC and ectopic miR-23b-3p repressed GC cell growth and invasion by targeting RAI14.

It has been shown that circRNAs can sponge miRNAs to regulate GC progression^{15–17}. Herein, we identified a novel circNFATC3, which might have the potential to bind with miR-23b-3p. Previous studies showed that NFATC3 can promote cancer stemness in oral/oropharyngeal squamous cell carcinomas²⁸ and inhibiting NFATC3 ameliorates colitis-associated colorectal cancer²⁹. Herein, we found that circNFATC3 gave rise to a RNase R resistance in GC cells and harbored a co-localization with miR-23b-3p in the cytoplasm. Knockdown of circNFATC3 repressed the colony formation and cell invasion. Moreover, we also found that circNFATC3 could act as a sponge of miR-23b-3p to upregulate RAI14, leading to GC growth.

Conclusion

Altogether, our findings indicated that upregulation of RAI14 and circNFATC3 or downregulation of miR-23b-3p was associated with poor prognosis in patients with GC. RAI14 regulated by circNFATC3/miR-23b-3p axis facilitated GC cell growth and invasion.

Author contributions

QZ, HW, and XJ designed this study. XY, MZ, and BL performed the experiments and contributed equally to this manuscript. XY wrote the paper and QZ revised the manuscript. All the authors read and approved the final manuscript.

XinXin Yan and MingZhi Zhang are two authors contributed equally to this article.

Data Accessibility

Data can be accessed by contacting first or corresponding author on demand.

Ethical Approval

Procedures performed in the study were in accordance with the ethical standards of the institutional research committee.

Statement of Human and Animal Rights

All of the experimental procedures involving animals were conducted in accordance with the guidelines from the Medical Ethics Committee of Tianjin Medical University General Hospital.

Statement of Informed Consent

There are no human subjects in this article and informed consent is not applicable.


Declaration of Conflicting Interests

The author(s) declared no potential conflicts of interest with respect to the research, authorship, and/or publication of this article.

Funding

The author(s) received the following financial support for the research, authorship, and/or publication of this article: the Foundation of Aerospace Center Hospital (YN202107).

ORCID iD

XinXin Yan  <https://orcid.org/0000-0002-5859-5719>

Supplemental Material

Supplemental material for this article is available online.

References

- Chen W, Zheng R, Zhang S, Zeng H, Zuo T, Xia C, Yang Z, He J. Cancer incidence and mortality in China in 2013: an analysis based on urbanization level. *Chin J Cancer Res.* 2017;29(1):1–10.
- Bang CS, Baik GH, Shin IS, Kim JB, Suk KT, Yoon JH, Kim YS, Kim DJ. Helicobacter pylori eradication for prevention of metachronous recurrence after endoscopic resection of early gastric cancer. *J Korean Med Sci.* 2015;30(6):749–756.
- Yasui W, Oue N, Aung PP, Matsumura S, Shutoh M, Nakayama H. Molecular-pathological prognostic factors of gastric cancer: a review. *Gastric Cancer.* 2005;8(2):86–94.
- Su X, Zhang J, Yang W, Liu Y, Liu Y, Shan Z, Wang W. Identification of the prognosis-related lncRNAs and genes in gastric cancer. *Front Genet.* 2020;11:27.
- Wei L, Sun J, Zhang N, Zheng Y, Wang X, Lv L, Liu J, Xu Y, Shen Y, Yang M. Noncoding RNAs in gastric cancer: implications for drug resistance. *Mol Cancer.* 2020;19(1):62.
- Yuan W, Zheng Y, Huo R, Lu L, Huang XY, Yin LL, Li JM, Zhou ZM, Sha JH. Expression of a novel alternative transcript of the novel retinal pigment epithelial cell gene NORPEG in human testes. *Asian J Androl.* 2005;7(3):277–288.
- Qian X, Mruk DD, Cheng CY. Rai14 (retinoic acid induced protein 14) is involved in regulating f-actin dynamics at the ectoplasmic specialization in the rat testis*. *PLoS One.* 2013;8(4):e60656.
- Hsu YC, Chen HY, Yuan S, Yu SL, Lin CH, Wu G, Yang PC, Li KC. Genome-wide analysis of three-way interplay among gene expression, cancer cell invasion and anti-cancer compound sensitivity. *BMC Med.* 2013;11:106.
- He XY, Zhao J, Chen ZQ, Jin R, Liu CY. High Expression of retinoic acid induced 14 (RAI14) in gastric cancer and its prognostic value. *Med Sci Monit.* 2018;24:2244–2251.
- Gu M, Zheng W, Zhang M, Dong X, Zhao Y, Wang S, Jiang H, Liu L, Zheng X. Downregulation of RAI14 inhibits the proliferation and invasion of breast cancer cells. *J Cancer.* 2019;10(25):6341–6348.

11. Shen X, Zhang J, Zhang X, Wang Y, Hu Y, Guo J. Retinoic acid-induced protein 14 (rai14) promotes mtor-mediated inflammation under inflammatory stress and chemical hypoxia in a u87 glioblastoma cell line. *Cell Mol Neurobiol.* 2019; 39(2):241–254.
12. Chen C, Maimaiti A, Zhang X, Qu H, Sun Q, He Q, Yu W. Knockdown of RAI14 suppresses the progression of gastric cancer. *Onco Targets Ther.* 2018;11:6693–6703.
13. Qu S, Zhong Y, Shang R, Zhang X, Song W, Kjems J, Li H. The emerging landscape of circular RNA in life processes. *RNA Biol.* 2017;14(8):992–999.
14. Zhang X, Wang S, Wang H, Cao J, Huang X, Chen Z, Xu P, Sun G, Xu J, Lv J, Xu Z. Circular RNA circNRIP1 acts as a microRNA-149-5p sponge to promote gastric cancer progression via the AKT1/mTOR pathway. *Mol Cancer.* 2019;18(1):20.
15. Wang S, Tang D, Wang W, Yang Y, Wu X, Wang L, Wang D. circLMTK2 acts as a sponge of miR-150-5p and promotes proliferation and metastasis in gastric cancer. *Mol Cancer.* 2019;18(1):162.
16. Zhang J, Hou L, Liang R, Chen X, Zhang R, Chen W, Zhu J. CircDLST promotes the tumorigenesis and metastasis of gastric cancer by sponging miR-502-5p and activating the NRAS/MEK1/ERK1/2 signaling. *Mol Cancer.* 2019;18(1):80.
17. Li RC, Ke S, Meng FK, Lu J, Zou XJ, He ZG, Wang WF, Fang MH. CiRS-7 promotes growth and metastasis of esophageal squamous cell carcinoma via regulation of miR-7/HOXB13. *Cell Death Dis.* 2018;9(8):838.
18. Rong D, Lu C, Zhang B, Fu K, Zhao S, Tang W, Cao H. CircPSMC3 suppresses the proliferation and metastasis of gastric cancer by acting as a competitive endogenous RNA through sponging miR-296-5p. *Mol Cancer.* 2019;18(1):25.
19. Fang J, Hong H, Xue X, Zhu X, Jiang L, Qin M, Liang H, Gao L. A novel circular RNA, circFAT1(e2), inhibits gastric cancer progression by targeting miR-548 g in the cytoplasm and interacting with YBX1 in the nucleus. *Cancer Lett.* 2019;44:2222–2232.
20. Zhang J, Liu H, Hou L, Wang G, Zhang R, Huang Y, Chen X, Zhu J. Circular RNA_LARP4 inhibits cell proliferation and invasion of gastric cancer by sponging miR-424-5p and regulating LATS1 expression. *Mol Cancer.* 2017;16(1):151.
21. Liu F, Hu L, Pei Y, Zheng K, Wang W, Li S, Qiu E, Shang G, Zhang J, Zhang X. Long non-coding RNA AFAP1-AS1 accelerates the progression of melanoma by targeting miR-653-5p/RAI14 axis. *BMC Cancer.* 2020;20(1):258.
22. Li G, Wu Z, Li X, Ning X, Li Y, Yang G. Biological role of microRNA-103 based on expression profile and target genes analysis in pigs. *Mol Biol Rep.* 2011;38(7):4777–4786.
23. He RQ, Wu PR, Xiang XL, Yang X, Liang HW, Qiu XH, Yang LH, Peng ZG, Chen G. Downregulated miR-23b-3p expression acts as a predictor of hepatocellular carcinoma progression: A study based on public data and RT-qPCR verification. *Int J Mol Med.* 2018;41(5):2813–2831.
24. An Y, Zhang Z, Shang Y, Jiang X, Dong J, Yu P, Nie Y, Zhao Q. miR-23b-3p regulates the chemoresistance of gastric cancer cells by targeting ATG12 and HMGB2. *Cell Death Dis.* 2015; 6(5):e1766.
25. Wang J, Xue H, Zhu Z, Gao J, Zhao M, Ma Z. Expression of serum exosomal miR-23b-3p in non-small cell lung cancer and its diagnostic efficacy. *Oncol Lett.* 2020;20(4):30.
26. Zhu R, Li X, Ma Y. miR-23b-3p suppressing PGC1 α promotes proliferation through reprogramming metabolism in osteosarcoma. *Cell Death Dis.* 2019;10(6):381.
27. Zhang J, Zhang Y, Tan X, Zhang Q, Liu C, Zhang Y. MiR-23b-3p induces the proliferation and metastasis of esophageal squamous cell carcinomas cells through the inhibition of EBF3. *Acta Biochim Biophys Sin (Shanghai).* 2018; 50(6):605–614.
28. Lee SH, Kieu C, Martin CE, Han J, Chen W, Kim JS, Kang MK, Kim RH, Park NH, Kim Y, Shin KH. NFATc3 plays an oncogenic role in oral/oropharyngeal squamous cell carcinomas by promoting cancer stemness via expression of OCT4. *Oncotarget.* 2019;10(23):2306–2319.
29. Lin Y, Koumba MH, Qu S, Wang D, Lin L. Blocking NFATc3 ameliorates azoxymethane/dextran sulfate sodium induced colitis-associated colorectal cancer in mice via the inhibition of inflammatory responses and epithelial-mesenchymal transition. *Cell Signal.* 2020;74:109707.